Electric Power Systems Research xxx (2016) xxx–xxx

Contents lists available at ScienceDirect

Electric Power Systems Research

journal homepage: www.elsevier.com/locate/epsr

ARIMA-based decoupled time series forecasting of electric vehicle charging demand for stochastic power system operation

M. Hadi Amini[a,b,c,d], Amin Kargarian[e,**], Orkun Karabasoglu[a,b,c,d,*]

[a] Sun Yat-Sen University-Carnegie Mellon University Joint Institute of Engineering, Guangzhou, Guangdong 510006, China
[b] Department of Electrical and Computer Engineering, Carnegie Mellon University, Pittsburgh, PA 15213, USA
[c] SYSU-CMU Shunde International Joint Research Institute, Shunde, China
[d] School of Electronics and Information Technology, SYSU, Guangzhou, China
[e] Department of Electrical and Computer Engineering, Louisiana State University, Baton Rouge, USA

ARTICLE INFO

Article history:
Received 9 February 2016
Received in revised form 6 May 2016
Accepted 1 June 2016
Available online xxx

Keywords:
Demand forecasting
Charging demand
Electric vehicle parking lots
Autoregressive integrated moving average (ARIMA)
Chance-constrained security-constrained unit commitment

ABSTRACT

Large-scale utilization of electric vehicles (EVs) affects the total electricity demand considerably. Demand forecast is usually designed for the seasonally changing load patterns. However, with the high penetration of EVs, daily charging demand makes traditional forecasting methods less accurate. This paper presents an autoregressive integrated moving average (ARIMA) method for demand forecasting of conventional electrical load (CEL) and charging demand of EV (CDE) parking lots simultaneously. Our EV charging demand prediction model takes daily driving patterns and distances as an input to determine the expected charging load profiles. The parameters of the ARIMA model are tuned so that the mean square error (MSE) of the forecaster is minimized. We improve the accuracy of ARIMA forecaster by optimizing the integrated and auto-regressive order parameters. Furthermore, due to the different seasonal and daily pattern of CEL and CDE, the proposed decoupled demand forecasting method provides significant improvement in terms of error reduction. The impact of EV charging demand on the accuracy of the proposed load forecaster is also analyzed in two approaches: (1) integrated forecaster for CEL + CDE, and (2) decoupled forecaster that targets CEL and CDE independently. The forecaster outputs are used to formulate a chance-constrained day-ahead scheduling problem. The numerical results show the effectiveness of the proposed forecaster and its influence on the stochastic power system operation.

1. Introduction

Large-scale utilization of electric vehicles (EVs) significantly affects the overall load profile in future power systems. EVs are emerging as more economic and environmentally-friendly alternatives to the conventional fossil fuel-based cars. According to the announcement from the White House and the U.S. Department of Energy, reducing the cost of battery technologies will speed up the growing trend of EVs' sales [1]. Renewable energy resources, demand responsive loads, and distributed generation units such as EVs pave the road for future power systems to improve asset utilization and preserve an acceptable level of reliability [2,3]. In the literature, EVs have been considered as advantageous resources to improve power system operation [4]. They can act as flexible energy storage resources and participate in ancillary services procurement [5]. Consequently, plug-in electric vehicles can provide distributed dispatchable energy storages for smart grids [6]. In this context, the impact of optimal control of distributed energy storage systems on the electricity demand is analyzed for smart grids [7]. With greater usage of electric vehicles (EVs) among the urban drivers, the distribution grid will be subjected to larger stress due to surges in the demand of electricity for charging necessities of EVs [8].

Despite the numerous advantages of EV utilization, there also exist some issues caused by EVs. Forthcoming advantages and drawbacks of high penetration of EVs in power systems are investigated in [9,10]. In [11], a multi-objective optimization problem is modeled for the allocation of EV charging stations in the distribution networks. Moreover, authors in [12] take it one step further

* Corresponding author at: Sun Yat-sen University–Carnegie Mellon University Joint Institute of Engineering (JIE), School of Electronics and Information Technology, SYSU, Guangzhou, Guangdong, China; Scott Institute for Energy Innovation, Carnegie Mellon University, Pittsburgh, PA, USA; SYSU-CMU Shunde International Joint Research Institute, Guangdong, China. Tel.: +86 13226996631.
** Corresponding author at: Department of Electrical and Computer Engineering, Louisiana State University, Baton Rouge, USA.
E-mail addresses: amini@cmu.edu (M.H. Amini), kargarian@lsu.edu (A. Kargarian), karabasoglu@cmu.edu (O. Karabasoglu).

http://dx.doi.org/10.1016/j.epsr.2016.06.003
0378-7796/

Nomenclature

Indices, sets, and parameters

b	Index for bus
i	Index for generating unit
l	Index for line
t	Index for time period
ν	Index for electric vehicle (EV) class
C_b	Maximum battery capacity
chr	Charging rate
ϑ_ν	Market share of the νth EV class
d	Integrated (I) order of ARIMA
E_m	Energy consumption per mile driven
$F_i(\cdot)$	Production cost function of thermal unit i
M	Sufficiently large constant
$\overline{MD}$	Maximum drivable distance (with a fully-charged battery)
N	Auto-regressive (AR) order of ARIMA
L_i^r	Real load value at the ith hour
L_i^f	Forecast load value at the ith hour
$\Pr\{\cdot\}$	Probability measure
SF	Shift factor
RU_i, RD_i	Maximum ramp up/down rate of unit i, in MW/h
T_i^{on}, T_i^{off}	Minimum ON/OFF time of unit i, in hour
Z_x	$100\times(1-x)$th percentile of the standard normal distribution
μ_{ar}	Mean value of the arrival time being used for charging demand modeling
σ_{ar}	Standard deviation of arrival time being used for charging demand modeling
$\sigma_{b,t}$	Standard deviation of demand on bus b at time t which is provided by ARIMA forecaster
μ_d	Mean value of the departure time being used for charging demand modeling
σ_d	Standard deviation of EVs' departure time being used for charging demand modeling
μ_m	Mean value of lognormal distribution for probabilistic daily driven distance
σ_m	Standard deviation value of lognormal distribution for probabilistic daily driven distance being used for charging demand modeling
μ_{md}	Mean value of probabilistic daily driven distance being used for parking lot modeling
σ_{md}	Standard deviation of probabilistic daily driven distance being used for parking lot modeling
α_t, β_t	Confidence level of chance constraints at time t
$\underline{x}$, $\bar{x}$	Minimum and maximum of x
$\hat{x}$	Expected value of x

Variables

$D_{b,t}^k$	Demand of bus b at time t in day k
$\hat{D}_{b,t}^k$	Expected demand of bus b at time t in day k
$\hat{E}_d$	Expected energy demand of EV
$I_{i,t}$	Commitment state of unit i at time t
MD	Probabilistic daily driven distance
$P_{i,t}$	Generation of thermal unit i at time t
$PL_{l,t}$	Power flow in line l at time t
$R_{i,t}$	Reserve of thermal unit i at time t
RV_r	Standard normal random variable, i.e., a normal random variable with a mean of zero and a variance of one
SOC	Final state-of-charge of each electric vehicle in parking lot
$SUD_{i,t}$	Startup/shutdown cost of unit i at time t
$X_{i,(t-1)}^{on}$, $X_{i,(t-1)}^{off}$	ON/OFF time of unit i at time $t-1$, in hour
$\varepsilon_{b,t}^k$	Demand forecast error of bus b at time t in day k
τ_{ar}	Probabilistic arrival time
τ_d	Probabilistic departure time
τ_{dur}	Probabilistic charging duration

and present a two-stage model to allocate EV parking lots in the distribution systems considering power loss, network reliability, and voltage deviation. In [13], creating innovative smart charging facilities with effective communication networks among the utilities escorted by well-developed control infrastructures for the achievement of suitable grid stability and proper utilization of energy. The impact of different types of contract between EV aggregators and their customers on the electricity market behavior and social welfare are also presented in [14]. This paper examined the distribution networks criteria, including reliability index improvement, loss reduction, and cost optimization. However, the load forecasting error is considered neither in the optimization model nor in the power flow solution. In [3], plug-in electric vehicle (PEV) aggregator cooperated with DISCO to improve system reliability and participated in energy market transactions, while considering the behaviors of PEVs with respect to the introduced incentives. In [15], a comprehensive review of the issues related to large scale integration of EVs was provided. Aghaei et al. also studied the capabilities of EVs as an effective means to facilitate the integration of demand response programs and renewable energy sources into power systems [15]. In [4], the hourly coordination of EVs and wind power generation are taken into account to formulate a security-constrained unit commitment (SCUC) problem. This paper utilized EVs as distributed deferrable loads to reduce the volatility of wind power generations. However, the departure and arrival times of EVs are modeled in a deterministic manner. It is worth noting that the probabilistic model of EV charging demand and demand forecast uncertainty may not only affect decision-making procedures for power systems operation but also influence power systems planning problems.

Charging demand modeling and scheduling have been investigated in the literature. In [16], a stochastic model of EV charging demand was developed based on queuing theory. Darabi and Ferdowsi proposed an aggregated EV model to predict the total electricity demand [17]. This study considered four influential factors in the aggregation, i.e., EV types, driven distance, charging level, and charging starting time; the stochastic nature of EV charging demand and demand forecasting uncertainty are neglected. The impact of EVs' charging demand on distribution network is investigated in [18]. National household travel survey (NHTS) data is used to model the EVs charging demand. Deterministic electricity load profiles are used to evaluate the effect of EVs on distribution network. A smart load management scheme is addressed for coordination of plug-in EVs in [19]. This study is based on priority-charging time zones and considers the power network operational issues, e.g., voltage limits. The aforementioned studies have only been focused on EVs charging demand, but the uncertainty of demand forecasting has not been taken into account, i.e., demand is assumed to be deterministic.

Utilization of the EVs will increase the uncertainty of electricity demand, hence, we need more accurate forecasting methods to improve the system operation and performance [20]. Autoregressive integrated moving average (ARIMA) has been widely used for load forecasting purposes [21–25]. An accurate short-term demand forecasting method not only reduces operation costs,

Please cite this article in press as: M.H. Amini, et al., ARIMA-based decoupled time series forecasting of electric vehicle charging demand for stochastic power system operation, Electr. Power Syst. Res. (2016), http://dx.doi.org/10.1016/j.epsr.2016.06.003

but also improves the performance of the power systems, e.g., reliability improvement by preventive actions. A comprehensive review of time series approach for short-term forecasting is provided in [22]. In [23,24], artificial neural network (ANN)-based and hybrid ARIMA/ANN models were utilized to efficiently forecast electricity load. According to [25], evaluation of five different types of short-term load forecasting, which utilized demand data from ten European countries, ARIMA and principal component analysis (PCA) methods performed sufficiently. A single EV charging demand prediction based on sparse time series was proposed in [26]. This method utilized mobile application for the communication between EVs and charging stations. In [27], load forecast approaches and their role in demand side management was reviewed comprehensively. Furthermore, the effect of fast charging stations on load forecasting was studied in [28]. Korolko et al. utilizes a fractional ARIMA (fARIMA) model for demand prediction.

The EVs charging demand has a considerable impact on system scheduling and electricity markets. The system operator should consider the EVs charging demand, and its uncertainty to optimally provide adequate energy and reserve for the system [4]. More accurate model and demand forecast of the EVs can potentially benefit the market and decrease costs by reducing mismatches between day-ahead scheduling and real-time operation. The EVs charging uncertainty, which is modeled by distribution function in this paper, can be used for stochastic power system scheduling.

This paper presents an autoregressive integrated moving average (ARIMA) model to predict electric power consumption, including conventional electrical load (CEL) and charging demand of EVs (CDE). In the proposed EV parking lot model, we utilized probability density function (PDF) of arrival and departure times based on the historical data. In order to consider the driving pattern of different drivers, the expected driven distance values are calculated utilizing the PDF of daily driven distance data. The parameters of the proposed ARIMA model are adjusted based on the load point historical data to maintain the optimum root mean square (RMS) error. Regarding the χ^2 test, the RMS error stays constant for large **orders of Autoregressive (AR) models.**, hence we conclude that the error values in different days are uncorrelated and the error is a white noise. As the CEL and CDE might have different seasonal patterns, the impact of EVs' charging demand on the accuracy of the proposed load forecaster is investigated considering two strategies: an aggregated CEL + CDE forecaster and a decoupled CEL/CDE forecaster. The output of the proposed forecaster, which represents the PDF of forecasted demand, is used to formulate a chance-constrained based day-ahead scheduling problem with respect to uncertainties associated with CEL and CDE. Our main focus in this paper is the demand forecasting for transmission systems scheduling, while we have large-scale penetration of EVs in the distribution systems. Thus, we model the distribution system as a load and do not consider its detailed model. The flowchart of the proposed ARIMA-based time series forecasting for stochastic power system operation is illustrated in Fig. 1. Note that the detailed framework of the proposed forecaster is provided in Fig. 2.

Two test systems (6-bus and IEEE 24-bus test systems) are used to show the effectiveness of the proposed forecaster for the power system scheduling. To validate the forecaster proficiency for the day-ahead scheduling, the power system is rescheduled in real-time operation using the historical (real) data and the rescheduling cost is evaluated.

The rest of this paper is organized as follows. The proposed ARIMA-based demand forecasting model is presented in Section 2. Section 3 formulates a stochastic day-ahead market scheduling. Numerical results are illustrated in Section 4 followed by conclusions.

2. The proposed demand forecasting methodology

ARIMA-based demand forecaster is presented in this section which is able to achieve a highly accurate demand forecast.

2.1. Autoregressive integrated moving average

In order to introduce the ARIMA forecaster, we need to formulate the time series based on the time resolution of historical data. According to the availability of the historical data, we can formulate the ARIMA forecaster for various time steps. Assume that the average value of demand in kth day for bth bus is shown by $D^k_{b,t}$. The time series is constructed for the kth day using $ARIMA(N, d, 0)$ as shown in (1).

$$\left(1-\sum_{q=1}^{N} a_q (L)^q\right)(1-L)^d D^k_{b,t} = \varepsilon^k_{b,t} \forall b \quad \forall t = N+d, N+d+1, \ldots \tag{1}$$

where N and d are the auto-regressive and integrated orders of ARIMA model, respectively. a_q represents the parameters of autoregressive part of the model. L is the lag operator on arbitrary time series f_t such that $L^r f_t = f_{t-r}$. Based on (1), we can represent predicted demand for the tth time period as $D^k_{b,t} = \hat{D}^k_{b,t} + \varepsilon^k_{b,t}$, where $\hat{D}^k_{b,t}$ is the expected demand of bus b at hour t in day k, and $\varepsilon^k_{b,t}$ represents the corresponding forecast error. As an application of the proposed ARIMA-based forecaster, we plan to use the forecasted demand for stochastic day-ahead scheduling problem so that, in this paper, the time frame and time step are one day and one hour, respectively. Note that our proposed forecaster is not limited to a specific time step.

2.2. Electricity demand forecasting

Fig. 2 shows the three-step framework of ARIMA-based demand forecasting. Since the root-mean-square (rms) error stays constant for large auto-regressive orders, with respect to the χ^2 test, we conclude that the error values in different days are uncorrelated, and thus, the error is a white noise. Therefore, if $ARIMA(N, d, 0)$ is used for the prediction purposes, then the forecasting error is Gaussian white noise (GWN). In other words, random process f_t is a GWN of variance σ^2, i.e., $f_t \sim GWN(\sigma^2)$. Equivalently we can say $f_t \sim \mathcal{N}(0, \sigma^2)$ for every t. Note that the minimum obtained RMS error is the standard deviation.

The proposed approach adjusts ARIMA model parameters based on the historical data in the three following steps:

(a) Finding optimum integration order among three values, 1, 2, and 3. In the load forecasting for most of the cases $d = 1$ is the optimum integration order.
(b) Determination of appropriate auto-regressive order based on the total number of days available from the historical data.
(c) Calculation of mean square error to obtain white Gaussian noise's standard deviation.

2.3. Electric vehicle (EV) charging demand model

2.3.1. Probabilistic EV parking lots modeling

The charging demand of EVs is obtained using two probabilistic parameters: (1) expected driven distance, and (2) expected duration of charging.

(1) *Expected driven distance*: In this study, our goal is to estimate the day-ahead electricity load while considering the large-scale integration of EVs. In order to estimate the energy consumption

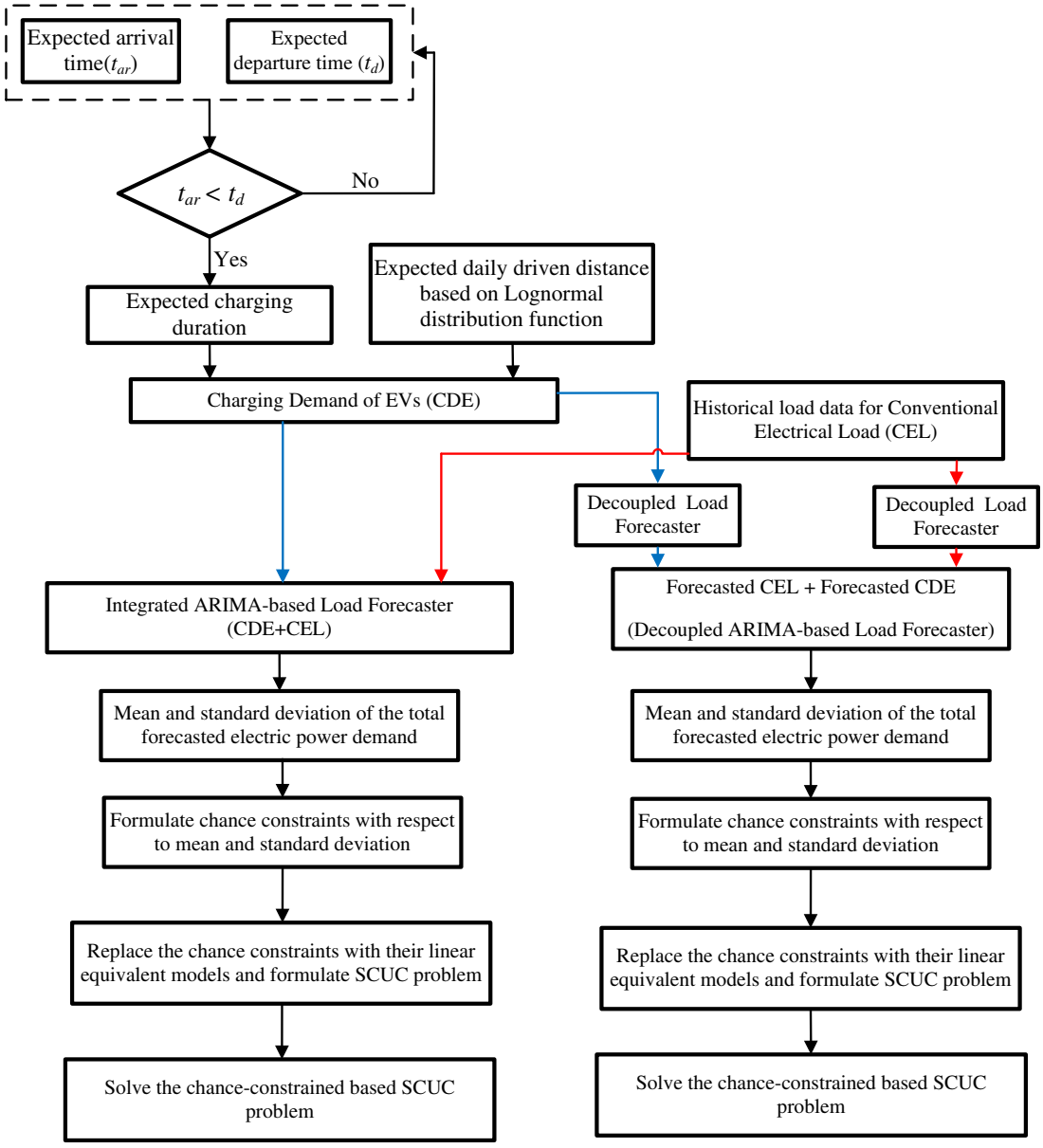

Fig. 1. Flowchart of the proposed method.

of EVs, we use reported fuel economy values and historical daily driven distance from [29]. Lognormal distribution function is utilized to generate the probabilistic daily driven distance, denoted as *MD* [29].

$$MD = e^{\mu_m + \sigma_m RV_r} \tag{2}$$

where RV_r is a standard normal value (a normal RV with a mean of zero and a variance of one), μ_m and σ_m are the lognormal distribution parameters and are obtained based on mean and standard variation of M_d using the historical data, denoted as μ_{md} and σ_{md}, respectively [30,31].

$$\begin{cases} \mu_m = \ln\left(\dfrac{\mu_{md}^2}{\sqrt{\mu_{md}^2 + \sigma_{md}^2}}\right) \\ \sigma_m = \sqrt{\ln\left(1 + \dfrac{\sigma_{md}^2}{\mu_{md}^2}\right)} \end{cases} \tag{3}$$

Based on the historical data of driving distance in [31], μ_{md} and σ_{md} are considered to be 40 miles and 20 miles, respectively. Maximum driving distance with a fully-charged battery, denoted by $\overline{MD}$, is calculated in (4).

$$\overline{MD} = \frac{C_b}{E_m} \tag{4}$$

where E_m is the energy consumption per miles driven, and C_b denotes the maximum battery capacity. The expected energy demand of the EV is calculated as shown in (5) [31].

$$\hat{E}_d = \begin{cases} C_b; & MD = \overline{MD} \\ MD \cdot E_m; & MD < \overline{MD} \end{cases} \tag{5}$$

(2) We also consider the expected charging duration as an effective parameter which depends on the charging rate (*chr*), battery capacity (C_b), as well as probabilistic arrival (τ_{ar}) and departure times (τ_d). In order to obtain the arrival time and departure time, the Gaussian distributions are used as the best estimate

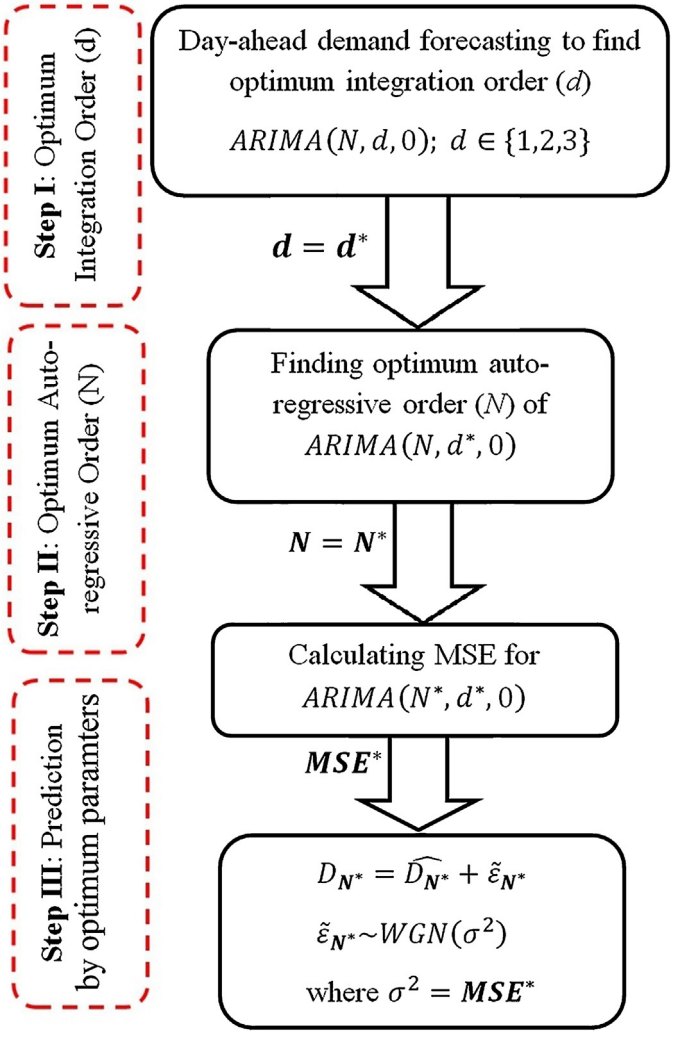

Fig. 2. Three-step framework of ARIMA-based demand forecasting.

of random residential consumer behavior. The probabilistic arrival and departure times are determined as:

$$\begin{cases} \tau_{ar} = \mu_{ar} + \sigma_{ar} \cdot RV_1 \\ \tau_d = \mu_d + \sigma_d \cdot RV_2 \end{cases} \quad (6)$$

where RV_1 and RV_2 represent two normally-distributed random variables, μ_{ar} and σ_{ar} show the mean and standard deviation of τ_{ar} based on the historical data, μ_d and σ_d are mean and standard variation of departure time, respectively. Arrival and departure times need to satisfy the following inequality: $\tau_d > \tau_{ar}$. If this constraint is not satisfied, another set of departure and arrival times should be generated. After generating the feasible probabilistic arrival and departure times, the probabilistic charging duration of each single EV can be calculated as:

$$\tau_{dur} = \tau_d - \tau_{ar} \quad (7)$$

Eventually, the charging demand of each EV can be calculated in terms of expected state-of-charge ($\widehat{SOC}$) using (8).

$$\widehat{SOC} = \min\left\{ \left[SOC_0 + \frac{\hat{E}_d}{C_b} \right], \left[SOC_0 + \frac{\tau_{dur} \cdot chr}{C_b} \right] \right\} \quad (8)$$

Table 1
EV classes specifications.

EV class, ν	C_b (kWh)	E_m (kWh/mile)	Market share, ϑ_ν (%)
1	10	0.3790	20
2	12	0.4288	30
3	16	0.5740	30
4	21	0.8180	20

Table 2
Charging rates.

Charging mode	Charging rate (chr)[a]
Slow charging	0.1
Medium charging	0.3
Fast charging	1.0

[a] Charging rates are given in battery capacity per hour.

2.3.2. Illustrative example

Tables 1 and 2 represent the characteristics of different EVs types and different available charging rates respectively. The parameters provided in Table 1 are extracted from [31]. EV classes 1, 2, 3, and 4 refer to micro car, economy car, mid-size car, and light truck/SUV respectively.

Here, we consider two cases to evaluate the effect of charging rate and different EV types on the charging demand.

Case 1: For a parking lot with capacity of 100 EVs, we evaluate the effect of different charging rates on the total charging demand. Note that the market share of different types of EVs is used based on Table 1. The effect of different charging rates on the total charging demand is presented in Fig. 3.
Case 2: For a fixed charging rate of 0.3, and fixed parking lot capacity of 100 EVs, we compare the effect of battery capacity on the total charging demand utilizing our EV parking lot model. Four penetration rates compared with the real market shares represented in Table 1, and are shown in Table 3.

Fig. 4 shows the charging demand for the five specified scenarios in Table 3.

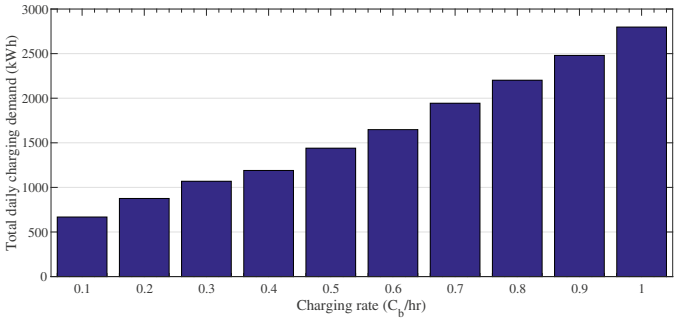

Fig. 3. The effect of charging rate on EV charging energy demand.

Table 3
Detailed specifications of the five evaluated scenarios.

Scenario index	Market shares of EV types (%)				Total daily charging demand (kWh)
	ϑ_1	ϑ_2	ϑ_3	ϑ_4	
Base scenario	20	30	30	20	982
S-I	80	10	5	5	829
S-II	10	80	5	5	857
S-III	5	5	80	10	1091
S-IV	5	5	10	80	1361

Please cite this article in press as: M.H. Amini, et al., ARIMA-based decoupled time series forecasting of electric vehicle charging demand for stochastic power system operation, Electr. Power Syst. Res. (2016), http://dx.doi.org/10.1016/j.epsr.2016.06.003

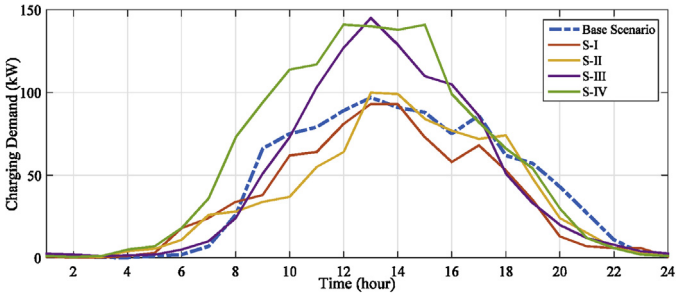

Fig. 4. Charging demand for different penetration rates of EV types.

3. Application of the proposed forecasting approach in the stochastic day-ahead scheduling

The probability distribution functions provided by the proposed ARIMA forecaster is used in the day-ahead scheduling problem. Outputs of the proposed forecasting approach can be also utilized in many power systems operation/planning problems. In this paper, we use a stochastic SCUC formulation to show how the outputs of the proposed forecaster is used. One can easily follow a similar procedure, and use the outputs of the proposed forecasting approach for other operation/planning purposes. Security-constrained unit commitment (SCUC) is one of the most important decision-making processes in the day-ahead scheduling [32,33]. In this section, a stochastic SCUC problem is formulated using the ARIMA forecaster outputs. The objective function is to minimize the production cost and the start up/shut down costs of generating units as follows:

$$Min \quad \sum_{\forall t}\sum_{\forall i} F_i(P_{i,t})I_{i,t} + SUD_{i,t} \tag{9}$$

The first term of the objective function is the production cost of the generating units, and the second term is the start up/shut down cost of the unit over the scheduling horizon (e.g., 24 h).

In addition to the uncertainty of conventional loads which is considered in [33–35], we also take the stochastic behavior of the electric vehicles into account, i.e., we consider the following parameters: (1) expected daily driven distance based on the historical data and (2) probabilistic arrival/departure time. In [34,35], Monte Carlo simulation is deployed to model the scenarios and then the stochastic security-constrained unit commitment problem is solved. In this paper, we utilize chance-constrained optimization to solve the SCUC problem. Using the probability distribution functions determined by the ARIMA forecaster for electricity demand and EV power consumption, the optimization constraints are formulated as in (10)–(18). Constraints (10)–(16) are deterministic, and (17) and (18) are stochastic constraints being modeled as chance constraints.

$$I_{i,t}\underline{P}_i \le P_{i,t} \le I_{i,t}\bar{P}_i \quad \forall i, \forall t \tag{10}$$

$$R_{i,t} = I_{i,t}\min\{\bar{R}_i, \bar{P}_i - P_{i,t}\} \quad \forall i, \forall t \tag{11}$$

$$P_{i,t} - P_{i,(t-1)} \le RU_i + M(2 - I_{i,(t-1)} - I_{i,t}) \quad \forall i, \forall t \tag{12}$$

$$P_{i,(t-1)} - P_{i,t} \le RD_i + M(2 - I_{i,(t-1)} - I_{i,t}) \quad \forall i, \forall t \tag{13}$$

$$\left(X^{on}_{i,(t-1)} - T^{on}_i\right)\left(I_{i,(t-1)} - I_{i,t}\right) \ge \quad \forall i, \forall t \tag{14}$$

$$\left(X^{off}_{i,(t-1)} - T^{off}_i\right)\left(I_{i,t} - I_{i,(t-1)}\right) \ge 0 \quad \forall i, \forall t \tag{15}$$

$$\sum_{\forall i} P_{it} = \sum_{\forall b} \hat{D}_{b,t} \quad \forall t \tag{16}$$

$$\Pr\left\{\sum_{\forall i}(P_{i,t} + R_{i,t}) \ge \sum_{\forall b} D_{b,t}\right\} \ge \alpha_t \quad \forall t \tag{17}$$

$$\Pr\left\{-\overline{PL_l} \le \sum_{\forall i} SF_{l,i}\cdot P_{i,t} - \sum_{\forall b} SF_{l,b}\cdot D_{b,t} \le \overline{PL_l}\right\} \ge \beta_{l,t} \quad \forall l, \forall t \tag{18}$$

where (10) represents upper and lower band of power output of generating units; equality constraint (11) is the reserve provided by generating units; units ramping up and down times are imposed by (12) and (13); minimum up/down time constraints are formulated by (14) and (15). Equality constraint (16) is power balance constraint. Note that the expected value of stochastic variables determined by the proposed ARIMA-based load forecaster, electricity demand and EVs power consumption, are used in this constraint. As there might be deviation from the expected values in the real-time system operation, chance constraint (17) is formulated to guarantee the availability of the adequate spinning reserve during the real-time dispatch. The confidence level of this chance constraint at time t is denoted by α_t. The network security is taken into account by chance constraint (18). This constraint ensures that the power flow in line l at time t is within its limit with a pre-specified confidence level β_{lt}. It should be noted that α_t and β_{lt} need to be appropriately set by the operator to make a trade-off between economics and reliability of the system operation [36].

3.1. Deterministic model of the chance constraints

In order to solve the above-mentioned day-ahead scheduling problem, the chance constraints need to be replaced by their equivalent deterministic model. The system operator needs to know the PDFs of the stochastic parameters/variables to formulate the deterministic equivalent model of chance constraints. The proposed ARIMA forecaster provides the PDFs of EVs charging demand and electric power demand as follows:

$$D_{b,t} = \hat{D}_{b,t} + \varepsilon_{b,t} \quad \forall b, \forall t \tag{19}$$

where:

$$\varepsilon_{b,t} \sim N(0, \sigma^2_{b,t}) \quad \forall b, \forall t$$

In (19), $\hat{D}_{b,t}$ is the expected value of electric power demand, including expected value of EVs power consumption, at bus b, at hour t. Variance $\sigma^2_{b,t}$ models the forecast errors. Using expected values and variances, the chance constraints (17) and (18) can be converted to the following linear inequality constraint [36–38].

$$\sum_{\forall i}(P_{i,t} + R_{i,t}) \ge \sum_{\forall b}\hat{D}_{b,t} + Z_{\alpha_t}\left[\sum_{\forall b}\sigma^2_{b,t}\right]^{0.5} \quad \forall t \tag{20}$$

$$\sum_{\forall i} SF_{l,i}\cdot P_{i,t} - \sum_{\forall b} SF_{l,b}\cdot \hat{D}_{b,t} + Z_{\beta_t}\left[\sum_{\forall b}(SF_{b,t}\cdot\sigma_{b,t})^2\right]^{0.5} \le \overline{PL_l} \quad \forall l, \forall t \tag{21}$$

Note that the standard deviations of probability distribution functions directly influence the optimal day-ahead scheduling. A larger standard deviation results in having a set of more restricted constraints, (20) and (21), and as a consequence, it increases the total operating cost. The smaller the standard deviations are, the less the operating cost can be achieved. Furthermore, having more accurate predictions reduces the rescheduling costs, which are required to be performed to make up for the deviations between

Please cite this article in press as: M.H. Amini, et al., ARIMA-based decoupled time series forecasting of electric vehicle charging demand for stochastic power system operation, Electr. Power Syst. Res. (2016), http://dx.doi.org/10.1016/j.epsr.2016.06.003

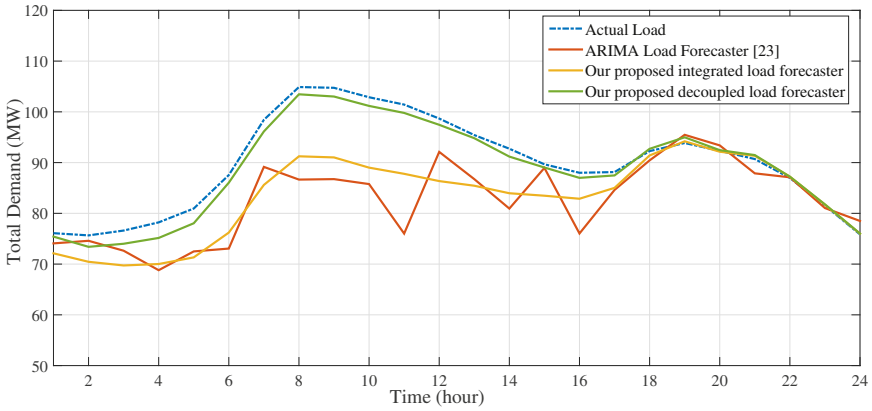

Fig. 5. Comparison of the integrated and decoupled methods [23].

Table 4
MAPE and MAE values for three different forecasting approaches.

Method	MAPE	MAE (MW)
ARIMA-based load forecasting method [23] ($\widehat{CEL+CDE}$)	8.04%	7.553
Our integrated load forecasting method ($\widehat{CEL+CDE}$)	7.25%	6.078
Our proposed decoupled load forecasting method ($\widehat{CDE}+\widehat{CEL}$)	1.44%	1.277

the pre-scheduled values (power produced by generating units) in the day-ahead market and the real-time operation. Therefore, the ARIMA forecaster (which defines the mean value and standard deviation) plays an important role on the total operating cost in the day-ahead scheduling problem. It should be noted that the expected values provided by the ARIMA model are used in the power balance constraint (16).

4. Numerical results

First, we provide the performance metrics to measure the accuracy of the proposed forecasting approach. The results are compared with the ARIMA forecaster used in [23]. Then, the effectiveness of the proposed ARIMA forecaster and its impact on the day-ahead system scheduling are studied on a six-bus and the IEEE 24-bus test systems. At first, the EV parking lots charging demand parameters are defined. A set of charging demand is generated based on the historical parameters. Based on the generated data and PJM historical metered load data, the load is forecasted using two different strategies as explained above: the aggregated CEL + CDE and the decoupled CEL/CDE. Then, the stochastic day-ahead scheduling is implemented using the forecasted data of these two forecasting strategies. Note that in order to emphasize and highlight the differences between the integrated and decoupled forecasters, we have considered a 10% EV energy charging demand penetration. Furthermore, the real-time system operation is performed with the real historical data. The rescheduling costs of both decoupled and integrated forecasting strategies are evaluated. The software code is written in MATLAB, and the computations are carried out using YALMIP toolbox [39] and ILOG CPLEX 12.4s MIQP solver on a 3.1 GHz personal computer.

4.1. Performance evaluation of the proposed forecasting approach

In order to validate the accuracy of the proposed forecaster, we use two widely-used metrics in the literature, mean absolute percentage error (MAPE) and mean absolute error (MAE). These metrics are defined respectively in (22) and (23).

$$\text{MAPE} = \sum_{i=1}^{N_f} \frac{e_i}{N_f} \tag{22}$$

$$\text{MAE} = \frac{1}{N_f} \sum_{i=1}^{N} \left| L_i^r - L_i^f \right| \tag{23}$$

where $e_i = \left| L_i^r - L_i^f \right| / L_i^r$, and N_f denoted the forecasting period.

We use the PJM load data to highlight the performance improvement of the utilized forecaster, and compared it with the forecasters presented in [23]. The number of EVs integrated is 12,000, with a charging rate of 0.3 of the battery capacity per hour. The average load demand is 80 MW. The load profile is extracted from PJM hourly metered load data by scaling down the total load to obtain the mentioned average demand. In our study, the forecasting period is 24 h (N_f = 24).

Table 4 represents the MAPE and MAE values for the three cases to validate the effectiveness of the proposed decoupled approach compared with both our integrated approach and the ARIMA-based forecasting method presented in [23].

According to the results, the accuracy of the proposed integrated forecaster is improved. Furthermore, considerable error reduction is observed for the decoupled load forecaster. The forecast load profiles of the three compared cases are presented in Fig. 5.

4.2. Case 1: the 6-bus test system

The 6-bus test system has 3 generation units, 7 lines, and 3 load points as shown in Fig. 6. Characteristics of the generation units and the network information are given in Tables 5 and 6, respectively. Loads 3, 4, and 5 consume 20%, 40%, and 40% of the total power demand of the system, respectively. In this case study, we assume that we have EV parking lots at buses 3, 4, and 5. The number of

Table 5
Generator data.

Unit	P_{max} (MW)	P_{min} (MW)	a (MBtu)	b (MBtu/MWh)	c (MBtu/(MW^2 h))	T^{off} (h)	T^{on} (h)	RU (MW/h)	RD (MW/h)
1	220	40	100	7	0.03	4	4	100	100
2	100	10	104	10	0.07	2	3	50	50
3	100	0	110	8	0.05	2	2	50	50

Please cite this article in press as: M.H. Amini, et al., ARIMA-based decoupled time series forecasting of electric vehicle charging demand for stochastic power system operation, Electr. Power Syst. Res. (2016), http://dx.doi.org/10.1016/j.epsr.2016.06.003

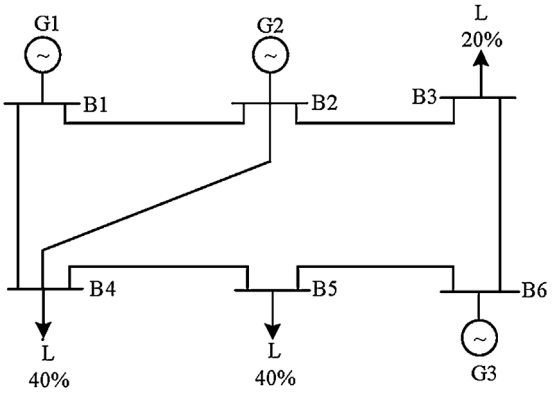

Fig. 6. Topology of the 6-bus test system.

Table 6
Network information.

From bus	To bus	X (pu)	Flow limit (MW)
1	2	0.170	200
1	4	0.258	200
2	3	0.037	190
2	4	0.197	200
3	6	0.018	180
4	5	0.037	190
5	6	0.140	180

Table 7
Statistical driving pattern parameters [31].

Parameter	μ_{ar}	σ_{ar}	μ_d	σ_d
Value	7	1.73	18	1.73

EVs at bus 3 is 10,000 EVs with the charging rate of 0.3 battery capacity per hour. The number of EVs at buses 4 and 5 is 12,000 with charging rate of 0.3 battery capacity per hour.

4.2.1. Electricity demand forecasting

Table 7 represents the typical values for parameters of driving pattern probability distribution function based on historical driving pattern data [31,40,41].

Typical values of these statistical parameters are extracted from [31], as shown in Table 7. Figs. 7 and 8 represent the results of demand forecasting for both CEL and CDE at the first load point (bus 3). Note that the total load in the analyzed 6-bus test system is 210 MW which is allocated to the buses. Note that to emphasize and highlight the differences between the integrated and decoupled forecasters, we have considered 10% EV energy charging demand penetration, i.e., the area below the conventional load demand over one day is 10% of the area below the EV charging demand curve over the same period of time.

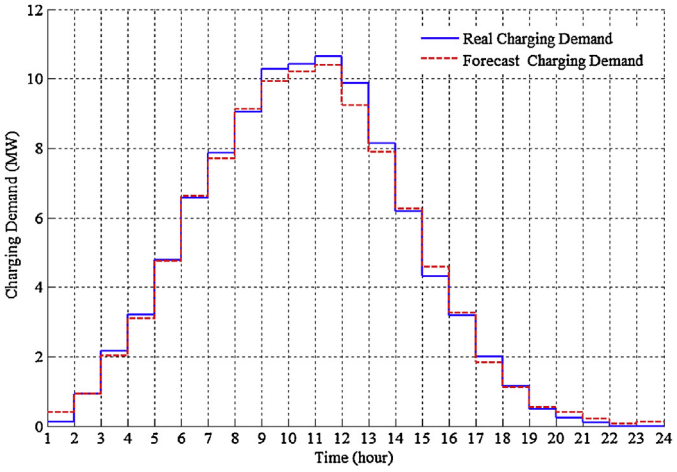

Fig. 8. Predicted CDE for bus 3.

According to Figs. 7 and 8, the predicted demand before EV integration (CEL) and the parking lots charging demand (CDE) are represented respectively. In order to find the integrated predicted load, we add the $\widehat{CDE}$ to $\widehat{CEL}$ for each time slot. Fig. 9 shows the results of the decoupled demand prediction obtained by adding the predicted *CDE* to the predicted *CEL*, i.e., $\widehat{CDE} + \widehat{CEL}$.

However the decoupled prediction of CEL and CDE leads to acceptable standard deviation values, and the integrated prediction has been also implemented to highlight the outperformance of the proposed decoupled prediction.

Fig. 10 demonstrates the results of integrated *CEL* and *CDE* prediction, i.e., $\widehat{CEL + CDE}$ for bus 3. According to this figure, the integrated forecasting approach will increase the error considerably. The different nature of the EV charging demand and conventional electricity demand is the important reason for this notable difference, i.e., *CDE* has daily load pattern while the *CEL* follows a seasonal pattern.

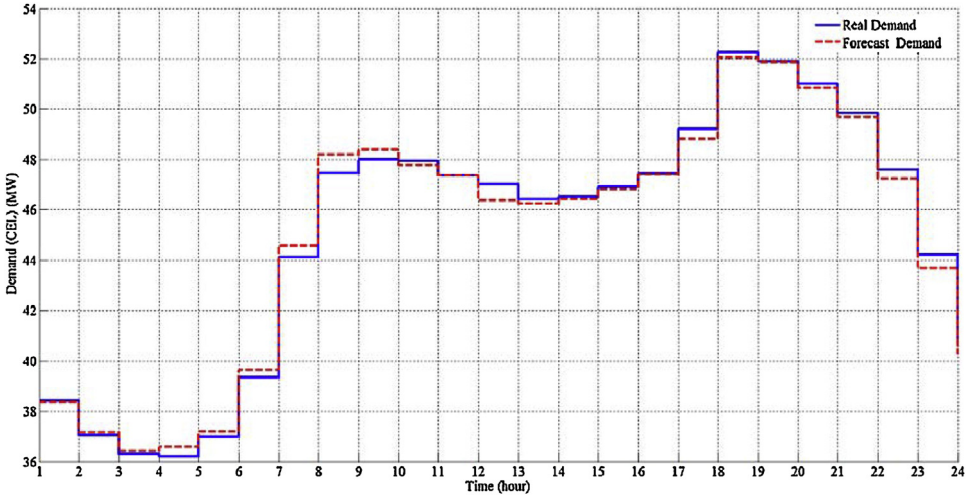

Fig. 7. Predicted CEL for bus 3.

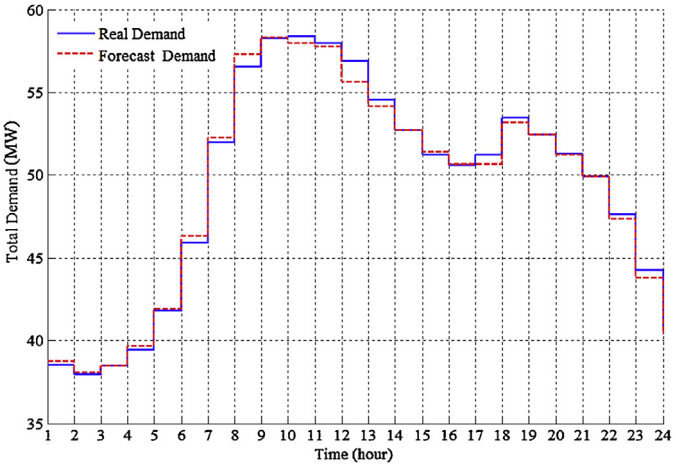

Fig. 9. Predicted *CEL* + predicted *CDE* for bus 3.

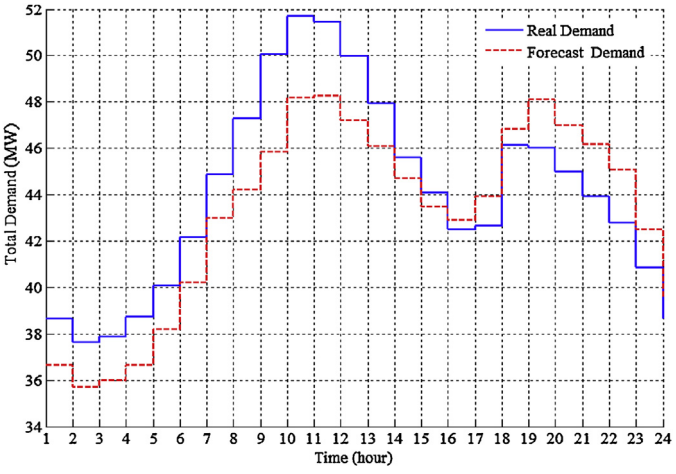

Fig. 10. Predicted $CEL + CDE$ ($\widehat{CEL + CDE}$) for bus 3.

In order to investigate the effect of number of the utilized EVs on the forecasting mean square error (MSE), the MSE error for both integrated and decoupled methods has been plotted for different number of EVs. Fig. 11 represents the results at bus 1.

According to this figure, the decoupled forecasting approach outperforms the integrated forecasting for all analyzed numbers of EVs in terms of the MSE values. Hence, from the demand forecasting point of view the decoupled forecasting method is more accurate. Henceforth, we evaluate the effect of these two forecasting strategies on the stochastic operation of power systems by considering two different test systems.

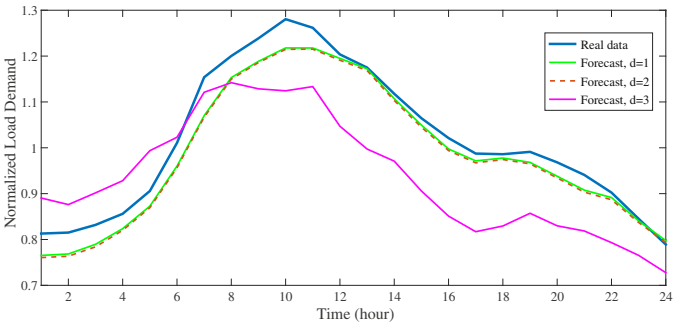

Fig. 12. Evaluating the effect of integration order on the forecasting accuracy.

Here we evaluate the effect of parameter tuning on the accuracy of the ARIMA forecaster. To this end we perform sensitivity analysis on both autoregressive and integration order parameters and provide the results. The utilized ARIMA model is different from the previous ARIMA models in terms of tuning the parameters to improve the performance of our forecaster which is applicable to EV charging demand prediction. The main reason to improve the forecasting accuracy is to utilize the decoupled forecasting strategy.

As it has been shown in Fig. 2, we adjust autoregressive order and integration order as two steps for parameter tuning to improve accuracy of the ARIMA model. Fig. 12 shows the effect of adjusting integration order, d, on the forecasting accuracy. The MSE values for $d = 1$, $d = 2$, and $d = 3$ are 0.037, 0.043, and 0.138 respectively. Note that these results are based on normalized load data on the unit scale, i.e., the mean of utilized data set is scaled to one, in order to facilitate the comparison between different cases.

As this figure shows, different values of integration order will lead to different forecasting accuracy levels. Hence, we tune d by evaluating the three mentioned values and choose the one with the least error. We also evaluated the effect of autoregressive order on the forecasting accuracy, by changing the value of N from 20 to 90. Fig. 13 represents the results.

From the results of Figs. 8 and 9, it can be seen utilizing tuned parameters for ARIMA forecaster will significantly increase the accuracy.

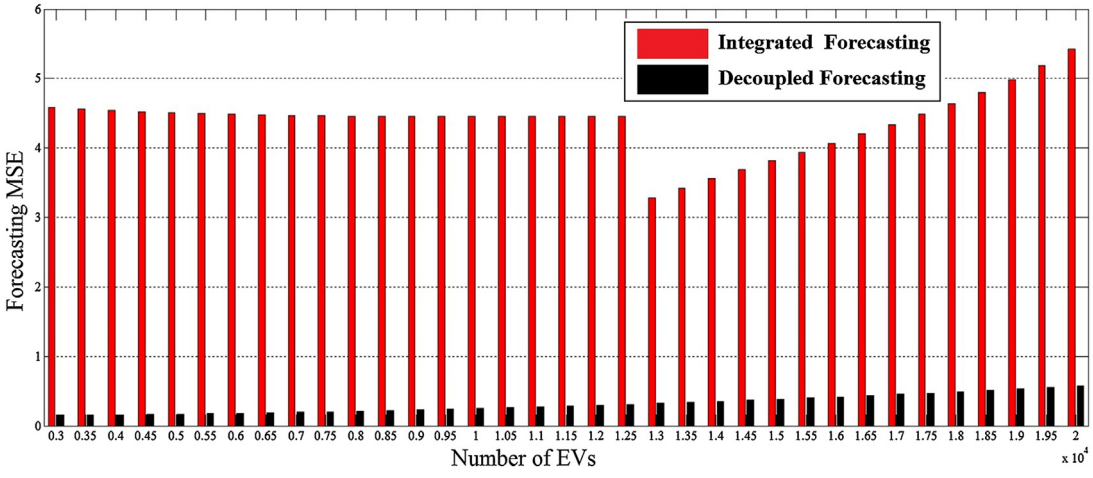

Fig. 11. Forecasting MSE for integrated and decoupled methods.

Please cite this article in press as: M.H. Amini, et al., ARIMA-based decoupled time series forecasting of electric vehicle charging demand for stochastic power system operation, Electr. Power Syst. Res. (2016), http://dx.doi.org/10.1016/j.epsr.2016.06.003

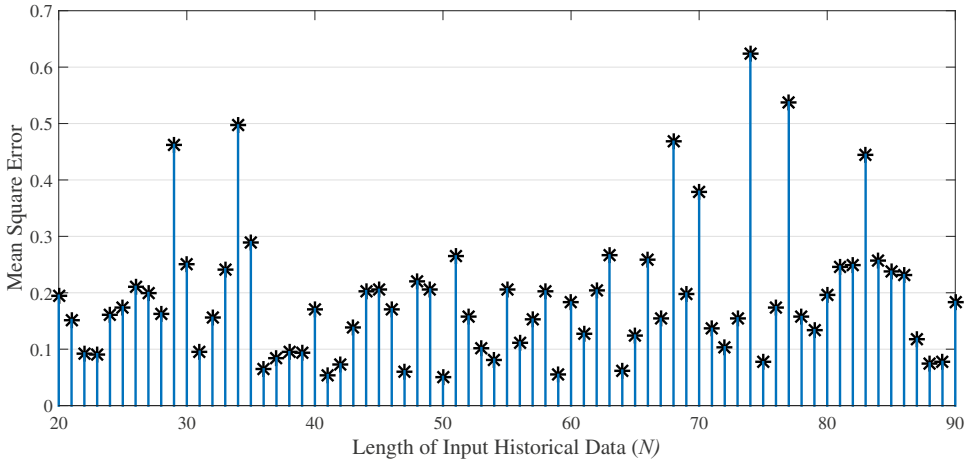

Fig. 13. Evaluating the effect of autoregressive order on the forecasting accuracy.

Table 8
UC solution for the aggregated CEL + CDE forecasting strategy.

Units	Hours (1–24)																							
1	1	1	1	1	1	1	1	1	1	1	1	1	1	1	1	1	1	1	1	1	1	1	1	1
2	0	0	0	0	0	1	1	1	1	1	1	1	1	1	1	1	1	1	1	1	1	1	0	0
3	1	1	1	1	1	1	1	1	1	1	1	1	1	1	1	1	1	1	1	1	1	1	1	1

Table 9
Day-ahead generation dispatch (MW) for the aggregated CEL + CDE strategy.

Hour	Unit1	Unit2	Unit3
1	130.60	0	68.36
2	129.69	0	67.81
3	130.94	0	68.56
4	137.71	0	72.62
5	142.79	0	75.68
6	133.96	35.98	70.38
7	153.57	44.39	82.14
8	161.13	47.63	86.68
9	160.12	47.19	86.07
10	149.81	42.78	79.89
11	150.04	42.87	80.02
12	141.91	39.39	75.15
13	139.74	38.46	73.84
14	137.58	37.54	72.55
15	132.49	35.35	69.50
16	130.98	34.71	68.59
17	132.81	35.49	69.69
18	136.94	37.26	72.16
19	138.36	37.87	73.01
20	133.65	35.85	70.19
21	133.92	35.97	70.35
22	130.74	34.60	68.44
23	136.41	0	71.85
24	132.31	0	69.39

4.2.2. Day-ahead scheduling

The stochastic day-ahead scheduling problem is solved using the forecasted conventional electrical load and charging demand of EVs, i.e., probability distribution functions obtained by the proposed ARIMA model in the previous section. The confidence levels (α_t and β_t) of both chance constraints (20) and (21) are set to 99% (99% and 95% are usually used in the literature for the confidence level).

Strategy one: SCUC with the aggregated CEL + CDE forecasting data ($\widehat{CEL + CDE}$). The unit commitment and generation dispatch results for the aggregated CEL + CDE forecasting strategy are shown in Tables 8 and 9. Generator 2, which is an expensive unit, is OFF during the off-peak load hours. This generator is committed to be OFF in 7 hours (hours 1, 2, 3, 4, 5, 23, 24). The other two generators are committed to be always ON to support the power demand over the scheduling horizon (i.e., 24 h). The total resulting day-ahead scheduling cost is $73,244.

Strategy two: SCUC with the decoupled CEL/CDE forecasting data ($\widehat{CDE} + \widehat{CEL}$). We resolve the SCUC using the decoupled CEL/CDE forecasting strategy. The unit status and generation dispatch results are represented in Table 10 and Table 11 respectively. Similar to Case A, generating units 1 and 3 are always ON, and unit 2 is ON when the power demand is close to peak hours. However, generating unit 2 is committed to be OFF at hour 22 unlike Case A where this unit is ON. In addition, the generation dispatch results of Case B are different from the one that determined in Case A. The total day-ahead scheduling cost in this case is $71,819, which is $1425 less than that obtained in Case A. These observations illustrate the difference between the hourly load predicted by the decoupled CEL/CDE and the aggregated CEL + CDE ARIMA-based forecasters.

4.2.3. Real-time system rescheduling

Due to the error between the day-ahead load prediction and the actual real-time power consumption, the operator needs to reschedule the system (modify the generating units output determined in day-ahead scheduling) to balance the generation and power consumption. We use the real hourly conventional electrical

Table 10
UC solution for the decoupled CEL/CDE forecasting strategy.

Units	Hours (1–24)																							
1	1	1	1	1	1	1	1	1	1	1	1	1	1	1	1	1	1	1	1	1	1	1	1	1
2	0	0	0	0	0	1	1	1	1	1	1	1	1	1	1	1	1	1	1	1	1	0	0	0
3	1	1	1	1	1	1	1	1	1	1	1	1	1	1	1	1	1	1	1	1	1	1	1	1

Table 11
Day-ahead generation dispatch (MW) for the decoupled CEL/CDE forecasting strategy.

Hour	Unit1	Unit2	Unit3
1	126.87	0	66.12
2	127.76	0	66.66
3	130.45	0	68.27
4	133.98	0	70.39
5	140.05	0	74.03
6	131.41	34.89	68.85
7	146.06	41.17	77.63
8	157.26	45.97	84.35
9	153.64	44.42	82.18
10	150.89	43.24	80.53
11	148.74	42.32	79.24
12	143.18	39.93	75.91
13	138.60	37.97	73.16
14	137.79	37.63	72.68
15	132.12	35.19	69.27
16	131.33	34.85	68.80
17	130.14	34.35	68.08
18	135.24	36.53	71.14
19	138.11	37.76	72.87
20	134.00	36.00	70.40
21	131.14	34.78	68.69
22	149.94	0	79.96
23	134.75	0	70.85
24	126.24	0	65.74

load and charging demand of EVs data (historical data) to evaluate the requirements for the system rescheduling. Two different types of day-ahead scheduling are performed: (1) using the aggregated CEL + CDE ARIMA-based forecaster ($\widehat{CEL + CDE}$) and (2) using the decoupled $\widehat{CEL} + \widehat{CDE}$. The system rescheduling is performed for both strategies, and the results are shown in Tables 12 and 13. The total resulting rescheduling cost of the aggregated CEL + CDE forecast strategy over the 24 h horizon is $2100. The total rescheduling cost of the decoupled strategy over the 24 h horizon is $1384. The results of rescheduling for 6-bus test network is represented in Table 14.

The total costs of the day-ahead scheduling and real-time system rescheduling using the aggregated strategy is $75,344. It is $73,203 when the operator uses the data obtained by the decoupled strategy, which is $2141 less than that of the aggregated strategy. Consequently, the proposed decoupled ARIMA-based forecaster provides a more accurate predictions of the conventional electrical load and charging demand of EVs, and using this data helps the operator to have a more accurate and efficient system scheduling.

Table 12
Real-time generation dispatch (MW) for aggregated CEL + CDE forecasting strategy.

Hour	Unit1	Unit2	Unit3
1	123.54	0	64.12
2	123.43	0	64.05
3	125.41	0	65.24
4	128.55	0	67.13
5	135.50	0	71.30
6	127.08	33.03	66.24
7	141.41	39.18	74.85
8	149.11	42.48	79.47
9	148.45	42.19	79.07
10	145.73	41.03	77.44
11	143.32	39.99	75.99
12	139.08	38.18	73.45
13	135.64	36.70	71.39
14	131.76	35.04	69.06
15	128.89	33.81	67.33
16	127.13	33.05	66.28
17	128.02	33.43	66.81
18	133.78	35.91	70.27
19	134.66	36.28	70.80
20	132.16	35.21	69.29
21	129.79	34.19	67.87
22	124.32	31.85	64.59
23	134.08	0	70.45
24	124.62	0	64.77

Table 13
Real-time generation dispatch (MW) for decoupled CEL/CDE forecasting strategy.

Hour	Unit1	Unit2	Unit3
1	123.54	0	64.12
2	123.43	0	64.05
3	125.41	0	65.24
4	128.56	0	67.13
5	135.50	0	71.30
6	127.08	33.03	66.24
7	141.41	39.18	74.85
8	149.12	42.48	79.47
9	148.45	42.19	79.07
10	145.73	41.03	77.44
11	143.32	39.99	75.99
12	139.08	38.18	73.45
13	135.65	36.70	71.38
14	131.77	35.04	69.06
15	128.89	33.81	67.33
16	127.13	33.05	66.27
17	128.02	33.43	66.81
18	133.78	35.91	70.27
19	134.67	36.28	70.80
20	132.16	35.21	69.29
21	129.79	34.19	67.87
22	144.22	0	76.53
23	134.08	0	70.45
24	124.62	0	64.77

4.3. Case 2: the IEEE 24-bus test system

We have applied the proposed forecasting approach on the IEEE 24-bus test system. The system has 10 generation units and 17 load points. In this case study, we assume that we have EV parking lots at buses 1, 3, 4, 6, 8, 10, 13, 15, 19, and 20. The number of EVs at buses 4, 10, 19, and 20 is 40,000 EVs with the charging rate of 0.3 battery capacity per hour. The number of EVs at buses 1 and 6 is 60,000 with charging rate of 0.3 battery capacity per hour. The number of EVs at buses 3, 8, 13, and 15 is 80,000 with charging rate of 0.3 battery capacity per hour.

The two forecasting strategy are applied to predict the load over the next 24 h. According to the forecasting results, the maximum standard deviation in the decoupled and integrated forecasting scenarios are 54.96628 MW (bus 18, hour 7) and 149.6969 MW (bus 13, hour 8) respectively. The confidence level of the chance constraints is set to 0.95 and the stochastic SCUC is solved. Table 11 shows the day-ahead scheduling costs of the proposed decoupled and the integrated strategies. The day-ahead costs of the decoupled and integrated forecast strategies are $2,030,868 and $2,613,868, respectively. The proposed decoupled ARIMA-based forecaster ends up with a cost reduction of $583,000 compared with the integrated strategy.

Table 14
Simulation results for 6-bus test system.

Test system	6-bus test system	
Scenario	$\widehat{CEL + CDE}$	$\widehat{CDE} + \widehat{CEL}$
Run-time (s)	1	1
Day-ahead cost ($)	73,244	71,819
Rescheduling cost ($)	2100	1384
Total system cost = Day-ahead + Rescheduling cost ($)	75,344	73,203

Please cite this article in press as: M.H. Amini, et al., ARIMA-based decoupled time series forecasting of electric vehicle charging demand for stochastic power system operation, Electr. Power Syst. Res. (2016), http://dx.doi.org/10.1016/j.epsr.2016.06.003

Table 15
Simulation results for IEEE 24-bus test system.

Test system	24-bus test system	
Scenario	$\widehat{CEL+CDE}$	$\widehat{CDE}+\widehat{CEL}$
Run-time (s)	4	4
Day-ahead cost ($)	2,613,868	2,030,868
Rescheduling cost ($)	150,394	73,836
Total system cost = Day-ahead + Rescheduling cost ($)	2,764,262	2,104,704

Similar to Case 1, we also perform the system rescheduling in Case 2. The rescheduling costs of both forecasting strategies are shown in Table 15. This table also depicts the total daily operating costs (day-ahead scheduling cost + hourly rescheduling cost). The total costs of the decoupled strategy is 23.8% less than that obtained by the integrated strategy. This significant improvement validates the more accurate performance of the decoupled forecaster compared with the integrated forecaster.

According to case 1 (6-bus test system) and case 2 (IEEE 24-bus test system), we used the proposed forecasting approach to predict the power demand of each load point based on the historical data. We need a separate forecast for each load point rather than a joint forecast for all the loads. Hence the number of load points does not affect the accuracy of the proposed forecaster, as we deal with them separately. In other words, even if we have a very large-scale power system with many load points, the operator can use the proposed ARIMA-based forecasting approach to predict the power demand of each load point.

5. Conclusions

This paper proposes a time series based forecasting approach for charging demand of EV parking lots. This is accomplished via (1) improving the accuracy of ARIMA forecaster by tuning the integrated and auto-regressive order parameters, and (2) decoupling the daily charging demand profile of EV parking lots from the seasonally changing load profile. The case study demonstrates the considerable improvement of the demand forecaster performance, while we are using the decoupled forecaster instead of the integrated demand forecasting method. Our novel EV charging demand prediction model takes daily driving patterns and distances as the inputs to determine the expected charging load profiles. The forecaster outputs are used to formulate a chance-constrained day-ahead scheduling problem to show the potential cost saving benefits of the proposed forecaster in the security constrained unit commitment (SCUC) problem. The simulation results certify that the proposed decoupled CEL/CDE ARIMA-based forecaster leads to more accurate demand predictions compared with the traditional integrated forecasting strategy. This ultimately translates into a more effective unit commitment as well as power dispatch results, and reduces the total resulting operating cost, which is the sum of the day-ahead scheduling and the real-time rescheduling costs. According to the numerical results, the proposed forecaster with decoupled approach reduces the daily operating costs by almost 2.9% for the 6-bus test system and 23% for the IEEE-24 bus test system for the simulated scenario compared with the integrated forecasting approach. This can potentially lead to a considerable annual cost saving of $770k for the 6-bus system and $240M for the IEEE-24 bus system. Thus, when scaled, our demand forecasting approach might help achieve significant cost savings in stochastic power system operations.

Further research is required for investigating the effect of scheduled charging on the SCUC. This can be done by considering the scheduled charging within the formulation of chance constrained SCUC.

Acknowledgement

The authors would like to acknowledge the valuable inputs, fruitful comments, and discussions of Prof. Marija D. Ilić from Carnegie Mellon University to this article. The quality of this work is substantially improved by her comments. We also would like to thank Kritika Jain from SYSU-CMU Shunde International Joint Research Institute and Chengkun (George) Li for their effort in proofreading the manuscript.

References

[1] http://www.whitehouse.gov/the-press-office/2014/11/18/fact-sheet-growing-united-states-electric-vehicle-market.
[2] C.W. Gellings, The Smart Grid: Enabling Energy Efficiency and Demand Response, Fairmont Press, 2009.
[3] M. Rahmani-andebili, G.K. Venayagamoorthy, SmartPark placement and operation for improving system reliability and market participation, Electr. Power Syst. Res. 123 (June (6)) (2015) 21–30.
[4] M.E. Khodayar, L. Wu, M. Shahidehpour, Hourly coordination of electric vehicle operation and volatile wind power generation in SCUC, IEEE Trans. Smart Grid 3 (3) (2012) 1271–1279.
[5] W. Kempton, J. Tomic, Vehicle-to-grid power fundamentals: calculating capacity and net revenue, J. Power Sources 144 (2005) 268–279.
[6] H. Lund, W. Kempton, Integration of renewable energy into the transport and electricity sectors through V2G, Energy Policy 36 (9) (2008) 3578–3587.
[7] M. Yazdani-Damavandi, M.P. Moghaddam, M.-R. Haghifam, M. Shafie-khah, J.P.S. Catalao, Modeling operational behavior of plug-in electric vehicles' parking lot in multi energy systems, IEEE Trans. Smart Grid 7 (1) (2016) 124–135.
[8] I. Rahman, P.M. Vasant, B. Singh, M. Singh, M. Abdullah-Al-Wadud, N. Adnan, Review of recent trends in optimization techniques for plug-in hybrid, and electric vehicle charging infrastructures, Renew. Sust. Energy Rev. 58 (2016) 1039–1047.
[9] W. Kempton, J. Tomić, Vehicle-to-grid power implementation: from stabilizing the grid to supporting large-scale renewable energy, J. Power Sources 144 (1) (2005) 280–294.
[10] J. Tomić, W. Kempton, Using fleets of electric-drive vehicles for grid support, J. Power Sources 168 (2) (2007) 459–468.
[11] M. Moradijoz, M.P. Moghadam, M.-R. Haghifam, E. Alishahi, A multi-objective optimization problem for allocating parking lots in a distribution network, Int. J. Electr. Power Energy Syst. 46 (2013) 115–122.
[12] N. Neyestani, M.Y. Damavandi, M. Shafie-khah, J. Contreras, J.P.S. Catalao, Allocation of plug-in vehicles' parking lots in distribution systems considering network-constrained objectives, IEEE Trans. Power Syst. 30 (5) (2015) 2643–2656.
[13] I. Rahman, P.M. Vasant, B.S.M. Singh, M. Abdullah-Al-Wadud, On the performance of accelerated particle swarm optimization for charging plug-in hybrid electric vehicles, Alexandria Eng. J. 55 (1) (2016) 419–426.
[14] M. Shafie-khah, M.P. Moghaddam, M.K. Sheikh-El-Eslami, M. Rahmani-Andebili, Modeling of interactions between market regulations and behavior of plug-in electric vehicle aggregators in a virtual power market environment, Energy 40 (1) (2015) 139–150.
[15] J. Aghaei, A. Esmaeel Nezhad, A. Rabiee, E. Rahimi, Contribution of plug-in hybrid electric vehicles in power system uncertainty management, Renew. Sust. Energy Rev. 59 (2016) 450–458.
[16] M. Alizadeh, A. Scaglione, J. Davies, K.S. Kurani, A scalable stochastic model for the electricity demand of electric and plug-in hybrid vehicles, IEEE Trans. Smart Grid 5 (March (2)) (2014) 848–860.
[17] Z. Darabi, M. Ferdowsi, Aggregated impact of plug-in hybrid electric vehicles on electricity demand profile, IEEE Trans. Sustain. Energy 2 (October (4)) (2011).
[18] S. Shafiee, M. Fotuhi-Firuzabad, M. Rastegar, Investigating the impacts of plug-in hybrid electric vehicles on power distribution systems, IEEE Trans. Smart Grid 4 (September (3)) (2013).
[19] S. Deilami, A.S. Masoum, P.S. Moses, M.A.S. Masoum, Real time coordination of plug-in electric vehicle charging in smart grids to minimize power losses and improve voltage profile, IEEE Trans. Smart Grid 2 (September (3)) (2011) 456–467.
[20] L. Hernandez, et al., A survey on electric power demand forecasting: future trends in smart grids, microgrids and smart buildings, IEEE Commun. Surv. Tutor. 16 (3) (2013) 1–36.
[21] M.Y. Cho, J.C. Hwang, C.S. Chen, Customer short term load forecasting by using ARIMA transfer function model, in: Proc. of International Conference on Energy Management and Power Delivery, 1995.
[22] M.T. Hagan, S.M. Behr, The time series approach to short term load forecasting, IEEE Trans. Power Syst. 2 (3) (1987) 785–791.
[23] A.A. El Desouky, M.M. Elkateb, Hybrid adaptive techniques for electric-load forecast using ANN and ARIMA, IEE Proc. Generat. Transm. Distrib. 147 (4) (2000).
[24] G.P. Zhang, Time series forecasting using a hybrid ARIMA and neural network model, Neurocomputing 50 (2003) 159–175.
[25] J.W. Taylor, P.E. McSharry, Short-term load forecasting methods: an evaluation based on European data, IEEE Trans. Power Syst. 22 (4) (2007) 2213–2219.

Please cite this article in press as: M.H. Amini, et al., ARIMA-based decoupled time series forecasting of electric vehicle charging demand for stochastic power system operation, Electr. Power Syst. Res. (2016), http://dx.doi.org/10.1016/j.epsr.2016.06.003

[26] M. Majidpour, C. Qiu, P. Chu, R. Gadh, H.R. Pota, Fast prediction for sparse time series: demand forecast of EV charging stations for cell phone applications, IEEE Trans. Ind. Informat. (2015).
[27] A. Raza Khan, et al., Load forecasting, dynamic pricing and DSM in smart grid: a review, Renew. Sust. Energy Rev. 54 (2016) 1311–1322.
[28] N. Korolko, et al., Modeling and forecasting self-similar power load due to EV fast chargers, IEEE Trans. Smart Grid (2015).
[29] S. Meliopoulos, Power System Level Impacts of Plug-in Hybrid Vehicles, Power Systems Engineering Research Center (PSERC), 2009.
[30] P. Sharer, R. Leydier, A. Rousseau, Impact of drive cycle aggressiveness and speed on HEVs fuel consumption sensitivity, Argonne National Lab, 2007 (Online). Available http://www.transportation.anl.gov/modeling_simulation/PSAT/psat_presentations.html.
[31] G. Li, X.-P. Zhang, Modeling of plug-in hybrid electric vehicle charging demand in probabilistic power flow calculations, IEEE Trans. Smart Grid 3 (March (1)) (2012).
[32] A. Kargarian, Y. Fu, Z. Li, Distributed security-constrained unit commitment for large-scale power systems, IEEE Trans. Power Syst. 30 (4) (2015) 1925–1936.
[33] A. Khodaei, M. Shahidehpour, S. Bahramirad, SCUC with hourly demand response considering intertemporal load characteristics, IEEE Trans. Smart Grid 2 (3) (2011) 564–571.
[34] L. Wu, M. Shahidehpour, T. Li, Stochastic security-constrained unit commitment, IEEE Trans. Power Syst. 22 (2) (2007) 800–811.
[35] M.M.R. Sahebi, S.H. Hosseini, Stochastic security constrained unit commitment incorporating demand side reserve, Int. J. Electr. Power Energy Syst. 56 (2014) 175–184.
[36] H. Wu, M. Shahidehpour, Z. Li, W. Tian, Chance-constrained day-ahead scheduling in stochastic power system operation, IEEE Trans. Power Syst. 29 (July (4)) (2014) 1583–1591.
[37] R. Henrion, Introduction to chance-constrained programming. Tutorial Paper for the Stochastic Programming Community Home Page, 2004.
[38] A. Prékopa, Stochastic Programming, Kluwer, Dordrecht, The Netherlands, 1995.
[39] J. Löfberg, YALMIP: a toolbox for modeling and optimization in MATLAB, in: Proc. IEEE International Symposium on Computer Aided Control Systems Design, September, 2004.
[40] M.H. Amini, M.P. Moghaddam, Probabilistic modelling of electric vehicles' parking lots charging demand, in: 21st Iranian Conference on Electrical Engineering (ICEE), 2013.
[41] M.H. Amini, A. Islam, Allocation of electric vehicles' parking lots in distribution network, in: IEEE PES 5th Innovative Smart Grid Technologies Conference (ISGT), 2014.

Please cite this article in press as: M.H. Amini, et al., ARIMA-based decoupled time series forecasting of electric vehicle charging demand for stochastic power system operation, Electr. Power Syst. Res. (2016), http://dx.doi.org/10.1016/j.epsr.2016.06.003